Published on 26 November 2015. Downloaded by RESEARCH CENTRE FOR ECO-ENVIRONMENTAL SCIENCES, CAS on 18/04/2016 04:08:11.

Catalysis Science & Technology

PAPER

View Article Online
View Journal | View Issue

Cite this: *Catal. Sci. Technol.*, 2016, 6, 2289

Influence of alkali metals on Pd/TiO_2 catalysts for catalytic oxidation of formaldehyde at room temperature†

Yaobin Li, Changbin Zhang, Hong He,* Jianghao Zhang and Min Chen

Received 10th September 2015,
Accepted 5th November 2015

DOI: 10.1039/c5cy01521a

www.rsc.org/catalysis

We previously observed that sodium (Na) addition had a dramatic promotion effect on Pd/TiO_2 catalysts for formaldehyde (HCHO) oxidation. In this study, a series of alkali metal (Li, Na, K, Cs) doped Pd/TiO_2 catalysts were prepared and tested for ambient temperature HCHO oxidation. The results showed that the doped alkali metals have a common promotion effect on the performance of the Pd/TiO_2 catalysts for HCHO oxidation under ambient temperature, which followed the order K > Cs > Na > Li. X-ray diffraction (XRD), Brunauer–Emmett–Teller (BET), CO chemisorption, Transmission Electric Microscopy (TEM), temperature-programmed reduction by H_2 (H_2-TPR), X-ray photoelectron spectroscopy (XPS) and temperature-programmed desorption by O_2 (O_2-TPD) methods were used to characterize the alkali metal doped catalysts to investigate the mechanism of the alkali metal promotion effect. The results showed that a negatively charged and well-dispersed Pd species was induced and stabilized by alkali metal addition, which facilitates the activation of chemisorbed oxygen, and then enhances the performance of alkali metal doped Pd/TiO_2 catalysts for room temperature HCHO destruction. The K–Pd/TiO_2 catalyst in particular possessed the highest Pd dispersion degree with active sites, attributing to the best activity in ambient temperature HCHO oxidation.

1. Introduction

Formaldehyde (HCHO) is recognized as a major indoor air pollutant, which is mainly emitted from consumer products and building/furnishing materials.[1] Long-term exposure to indoor air containing even very low concentrations of HCHO may be detrimental to human health, leading to serious health problems including nasal tumors, irritation of the mucous membranes of the eyes and respiratory tract, and skin irritation.[2,3] Increasingly, humans are paying more attention to indoor air pollutants, therefore, the effective abatement of indoor air HCHO is urgently needed to improve indoor air quality and reduce public health risk.

Over the past decades, four technologies including adsorption, photo-catalysis, plasma technology and catalytic oxidation were investigated for use in the removal of HCHO.[4–9] Among these methods, catalytic oxidation is known as the most promising method for HCHO removal, which could selectively decompose HCHO to harmless CO_2 and water at a low temperature without any secondary pollution.[10,11] For decades, researchers paid attention to conventional catalysts including metal oxides (Co, Ni, Mn, Ag)[3,12–20] and supported noble metal (Pt, Au, Pd, Rh) catalysts[21–33] for HCHO oxidation. A relatively high temperature is generally needed to completely oxidize HCHO using the metal oxide catalysts. In contrast, complete oxidation of HCHO can achieved on noble metal catalysts, such as Pt-, Au- and Pd-based catalysts, around room temperature.[21–24,27,31] Therefore, the supported noble metal catalysts are more suitable for indoor air HCHO purification.

Alkali metals can serve as electronic or textural promoters for catalysts in various catalytic processes[34] including NO[35] and CO oxidation,[36,37] CO hydrogenation[38] and the water-gas shift reaction.[39–41] Recently, we found that the performance of the Pt/TiO_2 catalysts for formaldehyde oxidation was dramatically improved by the addition of alkali metal ions (such as Li^+, Na^+ and K^+), which due to an atomically dispersed Pt species was induced and stabilized.[24] Then, we further reported that the performance of the Pd/TiO_2 catalysts for HCHO destruction under ambient conditions was also promoted by Na addition, which resulted from the fact that a negatively charged and well-dispersed Pd species was induced and stabilized by Na species addition.[31] Therefore, it is worth exploring whether other alkali metals (such as Li, K and Cs) also have a common promotion effect on the Pd/TiO_2 catalysts for HCHO oxidation.

State Key Joint Laboratory of Environment Simulation and Pollution Control, Research Center for Eco-Environmental Sciences, Chinese Academy of Sciences, Beijing, 100085, China. E-mail: honghe@rcees.ac.cn; Fax: 86 10 62849123; Tel: 86 10 62849123

† Electronic supplementary information (ESI) available. See DOI: 10.1039/c5cy01521a

Published on 26 November 2015. Downloaded by RESEARCH CENTRE FOR ECO-ENVIRONMENTAL SCIENCES, CAS on 18/04/2016 04:08:11.

In the present work, a series of alkali metal (Li, Na, K, Cs) doped Pd/TiO_2 catalysts were prepared and their HCHO performance were tested at low temperature. It was found that all the alkali metals enhanced the performance of the Pd/TiO_2 catalysts and the promotion effect followed the order K > Cs > Na > Li. Among them, the K–Pd/TiO_2 catalyst showed the best performance in ambient temperature HCHO oxidation. Based on the characterization results, the mechanism of the influence of alkali metals on Pd/TiO_2 catalysts was further elucidated.

2. Experimental

2.1. Catalyst preparation

1 wt% Pd/TiO_2 and alkali metal doped 1 wt% Pd/TiO_2 catalysts with the same alkali metal/Pd mole ratio were prepared by co-impregnation of TiO_2 (Degussa P25, BET surface area 59 m^2 g^{-1}) with aqueous $Pd(NO_3)_2$ (Sigma-Aldrich) and alkali metal nitrate of Li, Na, K, or Cs (Sinopharm Chemical Reagent Beijing Co., Ltd). After impregnation, the excess water was removed in a rotary evaporator at 60 °C. The samples were dried at 110 °C for 12 h and then calcined at 400 °C for 2 h. Before activity testing and characterization, the samples were reduced with H_2 at 350 °C for 30 min, and denoted as TiO_2, Pd/TiO_2, Li–Pd/TiO_2, Na–Pd/TiO_2, K–Pd/TiO_2 and Cs–Pd/TiO_2. The samples without pretreatment are denoted as TiO_2-fresh, Pd/TiO_2-fresh, Li–Pd/TiO_2-fresh, Na–Pd/TiO_2-fresh, K–Pd/TiO_2-fresh and Cs–Pd/TiO_2-fresh.

2.2. Catalyst characterization

X-ray diffraction (XRD), Brunauer–Emmett–Teller (BET), CO chemisorption, inductively coupled plasma optical emission spectrometry (ICP-OES), temperature-programmed reduction by H_2 (H_2-TPR), X-ray photoelectron spectroscopy (XPS) and temperature-programmed desorption by O_2 (O_2-TPD) were carried out and the methods and instruments for the characterization were the same as our previous work.[31] Typically, the C 1s peak (284.8 eV) was used to calibrate the binding energy (B. E.) values and the spectra are shown in Fig. S1 (ESI†). Transmission electron microscopy (TEM) was carried out on a Tecnai G2 F20 U-Twin field emission system operated at 200 kV.

2.3. Catalyst activity testing

The method and equipment for catalyst activity testing were the same as in our previous work.[31] Typically, the relative humidity was kept 30% balanced by helium. The total inlet flow rate was 100 mL min^{-1}, corresponding to a gas hourly space velocity (GHSV) of 190 000 h^{-1}. Measurements of the turnover frequency (TOF) were obtained in a separate experiment where the conversion of HCHO was kept below 30% by varying the inlet HCHO concentration and GHSV, with negligible heat and mass-transfer effects. The conditions of the TOF measurement are shown in Table S1 (ESI†).

3. Results

3.1. Activity test

The performance of Pd/TiO_2 and the Li-, Na-, K-, Cs-doped Pd/TiO_2 catalysts for HCHO oxidation was tested and the results are shown in Fig. 1. When the concentration of HCHO was 140 ppm, the Pd/TiO_2 catalyst exhibited about 30% HCHO conversion to CO_2 at 25 °C and achieved 100% conversion at around 125 °C. After doping with the alkali metals, the performance of the Pd/TiO_2 catalyst was dramatically enhanced. The Li–Pd/TiO_2 catalyst exhibited nearly 35% HCHO conversion at room temperature and achieved 100% conversion at around 100 °C, while the Na–, K– and Cs–Pd/TiO_2 catalysts achieved almost 100% HCHO conversion at 25 °C. When tested under harsh reaction conditions of 550 ppm HCHO and a GHSV of 640 000 h^{-1}, the HCHO conversion was around 20% for the Na–Pd/TiO_2 catalyst, while it was improved to around 43% and 60% for the Cs–Pd/TiO_2 and K–Pd/TiO_2 catalysts, respectively. According to the above results, the alkali metals all enhanced the performance of the Pd/TiO_2 catalyst for formaldehyde (HCHO) oxidation and the promotion effects appreciably depended on the nature of the doped alkali metals, following the order K > Cs > Na > Li.

3.2. Characterization of catalysts

3.2.1. Structural features of samples. The XRD patterns of Pd/TiO_2 and the alkali metal doped Pd/TiO_2 catalysts together with TiO_2-fresh are shown in Fig. 2. There was no Pd species (Pd^0, PdO) observed for any samples, which indicated that the Pd species were highly dispersed on the TiO_2 support. However, Pd loading was identified by ICP-OES, as listed in Table 1. The actual Pd loading on the catalysts is close to the nominal ones. The results of the specific surface area (S_{BET}), average pore size (d_p) and total pore volume of Pd/TiO_2 and alkali metal-doped Pd/TiO_2 catalysts together with fresh TiO_2 are listed in Table 1. Compared with the bare

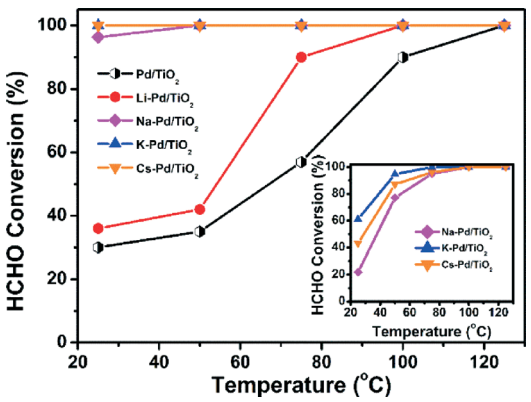

Fig. 1 HCHO conversion over Pd/TiO_2 and alkali metal (Li, Na, K, Cs) doped Pd/TiO_2 catalysts. Reaction conditions: 25 °C, 140 ppm HCHO, 20% O_2, 30% RH, He balance, GHSV 190 000 h^{-1} (inset: HCHO conversion over Na–, K– or Cs–Pd/TiO_2 catalysts at 25 °C with 550 ppm HCHO, GHSV 640 000 h^{-1} and the other conditions are the same).

This journal is © The Royal Society of Chemistry 2016

Published on 26 November 2015. Downloaded by RESEARCH CENTRE FOR ECO-ENVIRONMENTAL SCIENCES, CAS on 18/04/2016 04:08:11.

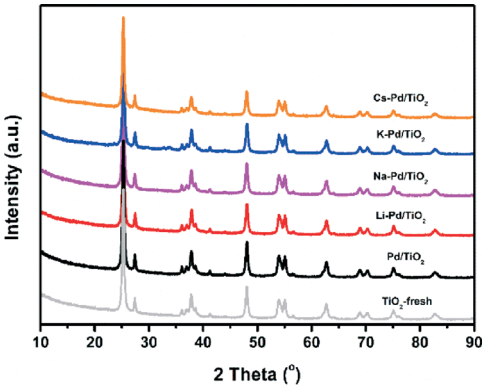

Fig. 2 XRD patterns of Pd/TiO_2 and alkali metal (Li, Na, K, Cs) doped Pd/TiO_2 catalysts together with fresh TiO_2 samples.

TiO_2, the S_{BET}, pore volume and d_p of the Pd/TiO_2, Li–, Na–, K–, and Cs–Pd/TiO_2 catalysts decreased to different degrees, which may be ascribed to diffusion of alkali metal species into the small pores of TiO_2.[42] In order to eliminate the influence of the surface area, the normalized reaction rate per unit area (R_s) at 25 °C with HCHO conversion kept below 60% was calculated and listed in Table 1. The R_s results also illustrated that all the alkali metal addition improved the performance of the Pd/TiO_2 catalyst for formaldehyde (HCHO) oxidation, which followed the order K > Cs > Na > Li.

3.2.2. Pd dispersion and particle size. Pd dispersion was measured by CO chemisorption and the results are listed in Table 1. Without alkali metal addition, the Pd dispersion was only 9.8%. With Li addition, the Pd dispersion increased slightly to 13.1%. In contrast, the Pd dispersion was remarkably increased to 32.9%, 40.6% and 48.2% by Na, Cs and K addition, respectively. It is clear that the alkali metals all improved the Pd dispersion, depending on the nature of the alkali metals. Based on the results of Pd dispersion, the TOFs were calculated at 25 °C. The value of TOF is 0.44×10^{-2} s^{-1} for the Pd/TiO_2 catalyst. After the alkali metal addition, it improved to 0.54×10^{-2} s^{-1}, 0.97×10^{-2} s^{-1}, 4.05×10^{-2} s^{-1} and 2.35×10^{-2} s^{-1} for the Li–, Na–, K– and Cs–Pd/TiO_2 catalysts, respectively. To directly show the Pd particle size on the catalysts, TEM was also carried out and the results are shown in Fig. S2† and Table 1. The TEM results indicated that the Pd particle size was obviously decreased after the alkali metal addition, which further confirmed that the alkali addition had a promotion effect on the Pd dispersion.

3.2.3. H_2-TPR. Fig. 3 shows the hydrogen temperature-programmed reduction (H_2-TPR) profiles conducted over the fresh TiO_2 and Li-, Na-, K- or Cs-doped TiO_2 (Fig. 3a) together with Pd/TiO_2 and the Li-, Na-, K- or Cs-doped Pd/TiO_2 catalysts (Fig. 3b) to study the reducibility of the catalysts. Pure TiO_2 exhibited no H_2 consumption peak from the −50 to 600 °C range, since TiO_2 reduction normally occurs at $T > 600$ °C.[22,43] There was a broad peak at 150–510 °C over Li/TiO_2, at 200–450 °C over Na/TiO_2, at 200–580 °C over K/TiO_2 and at 310–590 °C over Cs/TiO_2, which may be ascribed to the reduction of residual Li, Na, K and Cs nitrates, respectively. After Pd was loaded, a sharp PdO reduction peak appeared at around 0 °C on the Pd/TiO_2 catalysts.[44] With the further addition of alkali metals, the PdO reduction peak shifted to a higher temperature at about 47 °C over the Li–Pd/TiO_2 catalyst, at about 58 °C over Na–Pd/TiO_2 and Cs–Pd/TiO_2 catalysts and at about 70 °C over the K–Pd/TiO_2 catalyst. However, the reduction peak of alkali metal nitrates on the Li–Pd/TiO_2, Na–Pd/TiO_2, K–Pd/TiO_2 and Cs–Pd/TiO_2 catalysts shifted to 200–275, 113, 108 and 127 °C, respectively. The above results indicated an interaction between the alkali metal species and Pd species, which resulted in the alkali metal species stabilizing the PdO for the fresh catalysts and, after the PdO was reduced, the existence of the Pd metal species facilitated the reduction of the residual alkali metal nitrates.[39] Besides, also observed in the HR-TEM results of the Na–Pd/TiO_2 catalyst (see Fig. S2f†) is a partially covered Pd particle by NaO_x on the Na–Pd/TiO_2 catalyst, which further indicated the existence of the promoter–metal interaction.[39] In addition, the H_2 consumption of PdO on the samples was quantified and further converted to the Pd content. The results are shown in Table 1 which indicated that H_2 consumption was in agreement with expected Pd contents on the samples.

3.2.4. XPS analysis. The states of Pd, Ti and O on the catalyst surface were next identified with XPS measurements. Fig. 4 showed the XPS spectra of the catalysts and Table 2 summarized the binding energies and the percentages of

Table 1 Pd composition, specific surface area (BET), average pore size (d_p) and total pore volume of Pd/TiO_2 and alkali metal doped Pd/TiO_2 catalysts together with fresh TiO_2, Pd mean particle size, Pd dispersion (D_{CO}), TOF and normalized rate per unit area (R_s) for Pd/TiO_2 and alkali metal doped Pd/TiO_2 catalysts

Sample	Pd comp[a] (wt%)	Pd comp[b] (wt%)	BET (m^2 g^{-1})	d_p (nm)	Pore volume (cm^3 g^{-1})	Pd particle size (nm)	D_{CO}[c] (%)	TOF[d] ($\times 10^{-2}$ s^{-1})	R_s[e] (nmol s^{-1} m^{-2})
TiO_2-fresh			58.3	28.2	0.43				
Pd/TiO_2	0.95	1.11	53.1	28.7	0.38	6.1	9.8	0.44	2.0
Li–Pd/TiO_2	0.98	1.06	44.4	38.4	0.42	5.7	13.1	0.54	2.8
Na–Pd/TiO_2	0.98	1.07	56.9	31.7	0.40	4.7	32.9	0.97	5.2
K–Pd/TiO_2	0.97	1.08	53.6	31.5	0.42	3.4	48.2	4.05	19.3
Cs–Pd/TiO_2	0.96	1.02	48.7	30.1	0.37	4.2	40.6	2.35	17.7

[a] Pd composition was measured by ICP-OES. [b] Pd composition was calculated based on the H_2 consumption of PdO in H_2-TPR. [c] Dispersion of Pd measured by CO chemisorption. [d] TOF is calculated on the basis of D_{CO} with the HCHO conversion kept below 30%. The conditions are shown in Table S1 (ESI). [e] The amount of HCHO reacted per unit time and per unit area.

Published on 26 November 2015. Downloaded by RESEARCH CENTRE FOR ECO-ENVIRONMENTAL SCIENCES, CAS on 18/04/2016 04:08:11.

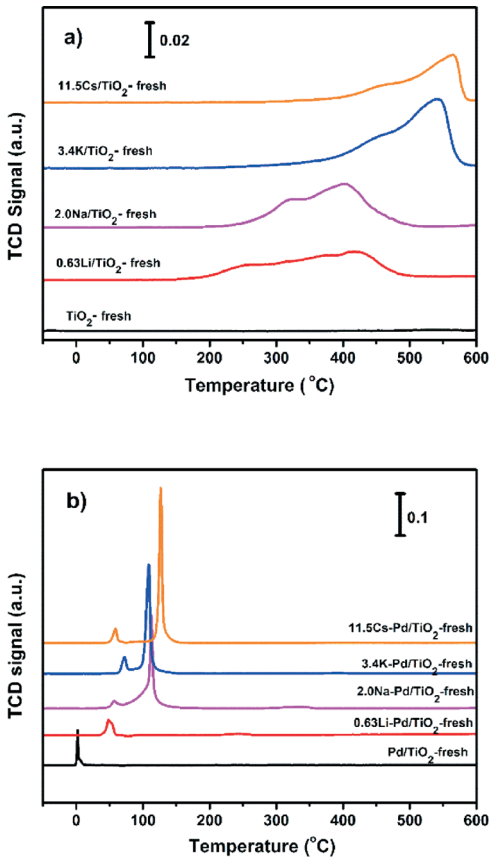

Fig. 3 H_2-TPR profiles of fresh samples: (a) TiO_2 and alkali metal (Li, Na, K, Cs) doped TiO_2; (b) Pd/TiO_2 and alkali metal (Li, Na, K, Cs) doped Pd/TiO_2 samples.

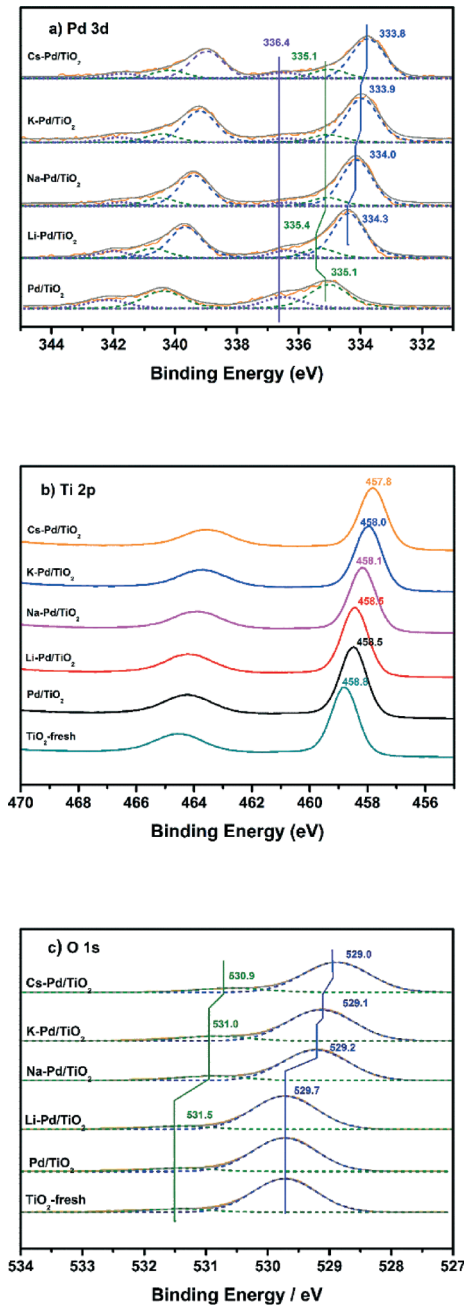

Fig. 4 XPS spectra of Pd/TiO_2 and alkali metal (Li, Na, K, Cs) doped Pd/TiO_2 catalysts together with TiO_2 sample: (a) Pd 3d, (b) Ti 2p and (c) O 1s.

calculated XPS peak areas. Based on Fig. 5a, the peak at 336.4 eV on all catalysts should be attributed to PdO,[45] which is due to re-oxidation of metallic Pd by O_2 and/or H_2O in air during transfer of the sample to the XPS chamber.[39] The peak at 335.4 eV on $Li–Pd/TiO_2$ and 335.1 eV on the other Pd/TiO_2 catalysts should be ascribed to metallic Pd.[46,47] With alkali metal addition, a third peak appeared at 334.3, 334.1, 333.9 and 333.8 eV over the Li–, Na–, K–, Cs–Pd/TiO_2 catalysts, respectively. These results clearly showed that the doped alkali metals, as electron donors, increased the electron density of Pd^0 by their interaction with metallic Pd,[48–50] and this electron donation effect became stronger with the increase in the atomic number of the alkali metal. In addition, according to the relative ratio of Pd species of the samples (Table 2), the negatively charged metallic Pd species were dominant on the alkali metal-doped Pd/TiO_2 catalyst surfaces, therefore playing the key role in HCHO oxidation under ambient temperature.

The Ti 2p peaks of the series of Pd/TiO_2 catalysts together with those of fresh TiO_2 are shown in Fig. 4b. The peak at 458.8 eV for the fresh TiO_2 catalyst was ascribed to Ti^{4+}.[29] A negative shift of 0.3 eV for Pd/TiO_2 occurred after Pd was loaded, which should be ascribed to partial reduction of TiO_2 during the H_2 pretreatment.[51] Compared with the Pd/TiO_2 catalyst, a further negative shift of 0.4, 0.5 and 0.7 eV occurred after Na, K, and Cs doping, respectively, which is attributed to electron transfer from the alkali metals to Ti and O of TiO_2[50] or may be partially attributed to further TiO_2 reduction caused by the alkali metal addition[52,53]

The O 1s XPS spectra of the catalysts are shown in Fig. 4c. All samples exhibited two kinds of O species. The main peak in the range of 529.7–529.0 eV was ascribed to the lattice oxygen of bulk TiO_2 (O_I), and the shoulder peak at 531.5–530.9 may be assigned to the Ti–OH species (O_{II}).[54] Table 2 shows the relative ratio of the Ti–OH species and lattice oxygen species, denoted as O_{II}/O_I. The ratio over the TiO_2-fresh, Pd/TiO_2 and $Li–Pd/TiO_2$ samples was about 0.10, while it increased to

 This journal is © The Royal Society of Chemistry 2016

Published on 26 November 2015. Downloaded by RESEARCH CENTRE FOR ECO-ENVIRONMENTAL SCIENCES, CAS on 18/04/2016 04:08:11.

Table 2 Pd 3d XPS data and the relative ratio of Pd species of Pd/TiO_2 and alkali metal doped Pd/TiO_2 catalysts, and the relative ratio of oxygen species

Sample	Pd 3d		O_{II}/O_I
	B. E. (eV)	Ratio (%)	
Pd/TiO_2	336.4	34.0	0.10
	335.1	66.0	
$Li–Pd/TiO_2$	336.4	12.3	0.11
	335.4	16.0	
	334.3	71.7	
$Na–Pd/TiO_2$	336.4	6.1	0.14
	335.1	14.4	
	334.0	79.5	
$K–Pd/TiO_2$	336.4	7.3	0.16
	335.1	13.6	
	333.9	79.1	
$Cs–Pd/TiO_2$	336.4	9.8	0.15
	335.1	13.9	
	333.8	76.3	

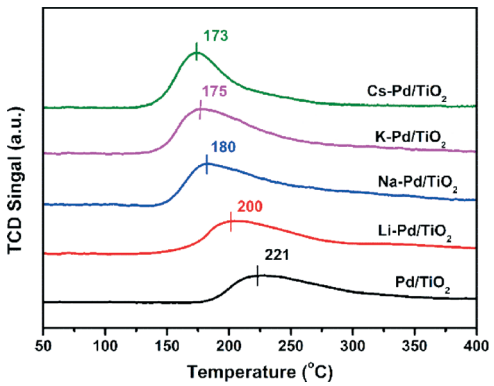

Fig. 5 O_2-TPD profiles of Pd/TiO_2 and alkali metal (Li, Na, K, Cs) doped Pd/TiO_2 samples. Conditions: the samples were pre-reduced with 10% H_2/Ar for 1 h at 350 °C, followed by purging with He and cooling down to 50 °C. Then the gas was switched to O_2 for adsorption for 30 min and He for purging for 1 h.

0.14, 0.16 and 0.15 with Na-, K- and Cs-doped Pd/TiO_2, respectively, indicating that Na, K and Cs addition may increase the concentration of surface OH groups.[55]

3.2.5. O_2-TPD. In order to investigate O_2 activation and mobility over the Pd/TiO_2 and alkali metal doped Pd/TiO_2 catalysts, O_2-TPD experiments were carried out and the results are shown in Fig. 5. Only one broad O_2 desorption peak between 50 °C and 400 °C appeared on all the Pd/TiO_2 samples. For the Pd/TiO_2 catalyst, the O_2 desorption peak was located at 221 °C. After alkali metal addition, the O_2 desorption peak shifted to lower temperatures, located at 200 °C for $Li–Pd/TiO_2$, 180 °C for $Na–Pd/TiO_2$ and about 175 °C for $K–Pd/TiO_2$ and 173 °C for $Cs–Pd/TiO_2$ catalysts, which indicated that alkali metal addition enhanced the mobility of the chemisorbed oxygen over the doped Pd/TiO_2 catalysts.

4. Discussion

As shown in Fig. 1, the alkali metals had a common promotion effect on the Pd/TiO_2 catalysts for HCHO oxidation, which followed the order K > Cs > Na > Li. Among them, the $K–Pd/TiO_2$ catalyst in particular possessed the best performance in HCHO oxidation under ambient temperature. Based on the characterization results, it is indicated that the promotion effect should be closely related to several factors, including Pd dispersion, the negatively charged metallic Pd, surface oxygen and OH species.

The S_{BET} results (Table 1) show that the S_{BET}, pore volume and d_p of the Pd/TiO_2, Li–, Na–, K–, and $Cs–Pd/TiO_2$ catalysts decreased to different degrees compared with the bare TiO_2. However, the R_s results were in line with the activities shown in Fig. 1, indicating that the reaction rates of the samples did not depend on their S_{BET}. As shown in Fig. 1 and Table 1, there is a correlation between the performance of the catalysts for HCHO oxidation and their Pd dispersion, indicating that the Cs, Na and K addition led to a significant improvement of Pd/TiO_2 catalyst performance by inducing more dispersed Pd species on the catalyst surface and exposing more Pd sites for HCHO oxidation. The improved Pd dispersion may be ascribed to the strong metal–promoter interaction, which can be observed from the results of H_2-TPR (Fig. 3). In addition, the interaction also had an effect on the electron density of metallic Pd. Based on Fig. 4a and Table 2, compared with the Pd/TiO_2 catalyst, negatively charged metallic Pd species were formed and were dominant on all the alkali metal doped samples. The alkali metal species, as electron donors, increase the electron density of Pd^0 through interaction with metallic Pd.[49] It has been reported that these negatively charged metallic Pd species could enhance O_2 adsorption through electron transfer from Pd metal to the antibonding π^* orbital of O_2.[29,56]

The results of Ti XPS (Fig. 4b) show that the alkali metal addition may facilitate the reduction of TiO_2. It has been reported that water could readily dissociate on TiO_2 defects to form OH groups,[57] which can be demonstrated by the results of O 1s XPS (Fig. 4c). The O 1s XPS results indicated that the concentrations of OH groups for the Na–, K–, and $Cs–Pd/TiO_2$ catalysts were enhanced after Na, K, and Cs addition. It has been reported that surface OH, on the one hand, can accelerate partial oxidation of HCHO to formate[24,26,28] and then facilely oxidize formate under ambient temperature;[24,26] on the other hand, the OH species can not only facilitate O_2 adsorption on the defects on TiO_2 (110) but also increase the diffusion of oxygen along the surface Ti (5c) to the alkali metal–Pd–TiO_2 interface.[58,59] The adsorbed oxygen was then activated by the negatively charged metallic Pd species and subsequently oxidized the adsorbed HCHO. There was little difference observed in the concentration of the surface OH groups and the mobility of chemisorbed O_2 for the Na-, K- and Cs-doped catalysts; however, the $K–Pd/TiO_2$ catalyst exhibited much higher TOFs (see Table 1) than the Na– and $Cs–Pd/TiO_2$ catalysts, which may be attributed to the smaller Pd particle size over $K–Pd/TiO_2$ catalyst with more metal–support interface. On the one hand, the adsorbed H_2O can easily dissociate into a surface OH group on oxygen vacancies,[57] especially in the proximity of the Pd particles at

Published on 26 November 2015. Downloaded by RESEARCH CENTRE FOR ECO-ENVIRONMENTAL SCIENCES, CAS on 18/04/2016 04:08:11.

the metal–support interface.[60] On the other hand, the dissociation of the molecularly adsorbed mobile oxygen may also take place at the metal–support interface.[60] The activated surface OH and O species play important roles in direct HCHO oxidation.[24]

5. Conclusions

The series of alkali metals show a common promotion effect on the Pd/TiO_2 catalyst for ambient temperature HCHO oxidation. The addition of Li, Na, K and Cs all could induce and stabilize a negatively charged metallic Pd species on the TiO_2 surface through the promoter–metal interaction, and then enhanced the chemisorption of surface oxygen species. Furthermore, the Na, K, and Cs addition could also induce more reaction sites by improving the Pd dispersion and number of surface OH groups, and enhance the mobility of chemisorbed oxygen. The K–Pd/TiO_2 catalyst in particular possessed the highest Pd dispersion and smaller Pd particles with more metal–support interfaces which facilitated chemisorption and dissociation of oxygen and formation of surface OH groups, contributing to its highest activity among the alkali metal doped catalysts.

Acknowledgements

This work was financially supported by the National Natural Science Foundation of China (51221892, 21422706, 21577159) and the Program of the Ministry of Science and Technology of China (2012AA062702).

Notes and references

1 J. Gunschera, S. Mentese, T. Salthammer and J. R. Andersen, *Build. Environ.*, 2013, **64**, 138–145.
2 G. D. Nielsen, S. T. Larsen and P. Wolkoff, *Arch. Toxicol.*, 2013, **87**, 73–98.
3 L. Ma, D. S. Wang, J. H. Li, B. Y. Bai, L. X. Fu and Y. D. Li, *Appl. Catal., B*, 2014, **148–149**, 36–43.
4 H. Q. Rong, Z. Y. Liu, Q. L. Wu, D. Pan and J. T. Zheng, *Cellulose*, 2009, **17**, 205–214.
5 J. C. Moreno-Pirajan, J. Tirano, B. Salamanca and L. Giraldo, *Int. J. Mol. Sci.*, 2010, **11**, 927–942.
6 F. Shiraishi, D. Ohkubo, K. Toyoda and S. Yamaguchi, *Chem. Eng. J.*, 2005, **114**, 153–159.
7 C. H. Ao and S. C. Lee, *Appl. Catal., B*, 2003, **44**, 191–205.
8 F. Holzer, U. Roland and F. D. Kopinke, *Appl. Catal., B*, 2002, **38**, 163–181.
9 M. B. Chang and C. C. Lee, *Environ. Sci. Technol.*, 1995, **29**, 181–186.
10 J. Quiroz Torres, S. Royer, J. P. Bellat, J. M. Giraudon and J. F. Lamonier, *ChemSusChem*, 2013, **6**, 578–592.
11 J. J. Pei and J. S. S. Zhang, *HVACR Res.*, 2011, **17**, 476–503.
12 C. Egawa, I. Doi, S. Naito and K. Tamaru, *Surf. Sci.*, 1986, **176**, 491–504.
13 B. Y. Bai, H. Arandiyan and J. H. Li, *Appl. Catal., B*, 2013, **142**, 677–683.
14 Y. R. Wen, X. Tang, J. H. Li, J. M. Hao, L. S. Wei and X. F. Tang, *Catal. Commun.*, 2009, **10**, 1157–1160.
15 X. F. Tang, Y. G. Li, X. M. Huang, Y. D. Xu, H. Q. Zhu, J. G. Wang and W. J. Shen, *Appl. Catal., B*, 2006, **62**, 265–273.
16 Z. P. Qu, S. J. Shen, D. Chen and Y. Wang, *J. Mol. Catal. A: Chem.*, 2012, **356**, 171–177.
17 S. Imamura, D. Uchihori, K. Utani and T. Ito, *Catal. Lett.*, 1994, **24**, 377–384.
18 J. Quiroz, J.-M. Giraudon, A. Gervasini, C. Dujardin, C. Lancelot, M. Trentesaux and J.-F. Lamonier, *ACS Catal.*, 2015, **5**, 2260–2269.
19 B. Y. Bai and J. H. Li, *ACS Catal.*, 2014, **4**, 2753–2762.
20 X. F. Tang, J. L. Chen, Y. G. Li, Y. Li, Y. D. Xu and W. J. Shen, *Chem. Eng. J.*, 2006, **118**, 119–125.
21 C. B. Zhang, H. He and K.-i. Tanaka, *Catal. Commun.*, 2005, **6**, 211–214.
22 C. B. Zhang, H. He and K.-i. Tanaka, *Appl. Catal., B*, 2006, **65**, 37–43.
23 C. B. Zhang and H. He, *Catal. Today*, 2007, **126**, 345–350.
24 C. B. Zhang, F. D. Liu, Y. P. Zhai, H. Ariga, N. Yi, Y. C. Liu, K. Asakura, M. Flytzani-Stephanopoulos and H. He, *Angew. Chem., Int. Ed.*, 2012, **51**, 9628–9632.
25 S. S. Kim, K. H. Park and S. C. Hong, *Appl. Catal., A*, 2011, **398**, 96–103.
26 D. W. Kwon, P. W. Seo, G. J. Kim and S. C. Hong, *Appl. Catal., B*, 2015, **163**, 436–443.
27 H. F. Li, N. Zhang, P. Chen, M. F. Luo and J. Q. Lu, *Appl. Catal., B*, 2011, **110**, 279–285.
28 B. B. Chen, C. A. Shi, M. Crocker, Y. Wang and A. M. Zhu, *Appl. Catal., B*, 2013, **132**, 245–255.
29 H. B. Huang and D. Y. C. Leung, *ACS Catal.*, 2011, **1**, 348–354.
30 E. Jeroro and J. M. Vohs, *J. Am. Chem. Soc.*, 2008, **130**, 10199–10207.
31 C. B. Zhang, Y. B. Li, Y. F. Wang and H. He, *Environ. Sci. Technol.*, 2014, **48**, 5816–5822.
32 S. Imamura, Y. Uematsu, K. Utani and T. Ito, *Ind. Eng. Chem. Res.*, 1991, **30**, 18–21.
33 Q. L. Xu, W. Y. Lei, X. Y. Li, X. Y. Qi, J. G. Yu, G. Liu, J. L. Wang and P. Y. Zhang, *Environ. Sci. Technol.*, 2014, **48**, 9702–9708.
34 W. D. Mross, *Catal. Rev.: Sci. Eng.*, 1983, **25**, 591–637.
35 S. S. Mulla, N. Chen, L. Cumaranatunge, W. N. Delgass, W. S. Epling and F. H. Ribeiro, *Catal. Today*, 2006, **114**, 57–63.
36 I. V. Yentekakis, G. Moggridge, C. G. Vayenas and R. M. Lambert, *J. Catal.*, 1994, **146**, 292–305.
37 B. Mirkelamoglu and G. Karakas, *Appl. Catal., A*, 2006, **299**, 84–94.
38 A. M. Kazi, B. Chen, J. G. Goodwin, G. Marcelin, N. Rodriguez and T. K. Baker, *J. Catal.*, 1995, **157**, 1–13.
39 X. L. Zhu, M. Shen, L. L. Lobban and R. G. Mallinson, *J. Catal.*, 2011, **278**, 123–132.
40 Y. P. Zhai, D. Pierre, R. Si, W. Deng, P. Ferrin, A. U. Nilekar, G. W. Peng, J. A. Herron, D. C. Bell, H. Saltsburg, M. Mavrikakis and M. Flytzani-Stephanopoulos, *Science*, 2010, **329**, 1633–1636.
41 M. Yang, S. Li, Y. Wang, J. A. Herron, Y. Xu, L. F. Allard, S. Lee, J. Huang, M. Mavrikakis and M. Flytzani-Stephanopoulos, *Science*, 2014, **346**, 1498–1501.

 This journal is © The Royal Society of Chemistry 2016

Published on 26 November 2015. Downloaded by RESEARCH CENTRE FOR ECO-ENVIRONMENTAL SCIENCES, CAS on 18/04/2016 04:08:11.

42 L. Xue, H. He, C. Liu, C. B. Zhang and B. Zhang, *Environ. Sci. Technol.*, 2009, **43**, 890–895.
43 N. S. de Resende, J.-G. Eon and M. Schmal, *J. Catal.*, 1999, **183**, 6–13.
44 H. Q. Zhu, Z. F. Qin, W. J. Shan, W. J. Shen and J. G. Wang, *J. Catal.*, 2004, **225**, 267–277.
45 K. Otto, L. P. Haack and J. E. deVries, *Appl. Catal., B*, 1992, **1**, 1–12.
46 H. Q. Yang, G. Y. Zhang, X. L. Hong and Y. Y. Zhu, *J. Mol. Catal. A: Chem.*, 2004, **210**, 143–148.
47 Q. Lin, Y. Ji, Z. D. Jiang and W. D. Xiao, *Ind. Eng. Chem. Res.*, 2007, **46**, 7950–7954.
48 L. F. Liotta, G. Deganello, P. Delichere, C. Leclercq and G. A. Martin, *J. Catal.*, 1996, **164**, 334–340.
49 L. F. Liotta, G. A. Martin and G. Deganello, *J. Catal.*, 1996, **164**, 322–333.
50 V. Pitchon, M. Guenin and H. Praliaud, *Appl. Catal.*, 1990, **63**, 333–343.
51 V. V. Rozanov and O. V. Krylov, *Russ. Chem. Rev.*, 1997, **66**, 117–130.
52 H. Onishi, T. Aruga, C. Egawa and Y. Iwasawa, *Surf. Sci.*, 1988, **199**, 54–66.
53 P. Panagiotopoulou and D. I. Kondarides, *J. Catal.*, 2009, **267**, 57–66.
54 L. H. Nie, J. G. Yu, X. Y. Li, B. Cheng, G. Liu and M. Jaroniec, *Environ. Sci. Technol.*, 2013, **47**, 2777–2783.
55 I. M. Brookes, C. A. Muryn and G. Thornton, *Phys. Rev. Lett.*, 2001, **87**, 2661031–2661034.
56 C. G. Vayenas, S. Bebelis, C. Pliangos, S. Brosda and D. Tsiplakides, *Electrochemical activation of catalysis: promotion, electrochemical promotion, and metal–support interactions*, Kluwer Academic Publishers/Plenum Press, New York, 2001, pp. 35–86.
57 Z. Zhang, O. Bondarchuk, B. D. Kay, J. M. White and Z. Dohnalek, *J. Phys. Chem. B*, 2006, **110**, 21840–21845.
58 H. B. Huang, X. G. Ye, H. L. Huang, L. Zhang and D. Y. C. Leung, *Chem. Eng. J.*, 2013, **230**, 73–79.
59 L. M. Liu, B. McAllister, H. Q. Ye and P. Hu, *J. Am. Chem. Soc.*, 2006, **128**, 4017–4022.
60 M. M. Schubert, S. Hackenberg, A. C. van Veen, M. Muhler, V. Plzak and R. J. Behm, *J. Catal.*, 2001, **197**, 113–122.